DOI: https://doi.org/10.67656/njmse.2018.kdhpdcje

Olawale et.al.: Nigerian Journal of Materials Science and Engineering.. Vol. 7A:1-9 (2017)

Quantitative Evaluation of Carbon-enriched Stabilised Austenite in Cast Austempered Ductile Iron of Varying Section Thickness

[*]**Olawale** John Oluyemi, **Ibitoye** Simeon Ademola and **Oluwasegun** Kunle Michael
Department of Materials Science and Engineering, Obafemi Awolowo University, Ile-Ife. Nigeria.

[*]Corresponding author: jooolawale@yahoo.com

Abstract

The quantity of carbon-enriched stabilised austenite (γHC) in austempered ductile iron (ADI) with various casting thicknesses was evaluated in this study. Ductile iron grade that conforms to ASTM A536 65-45-12 was cast, specimens of section thickness in the range of 5 to 25 mm were machined, isothermally treated to 820°C austenitising temperature, and austempered at austempering temperature (T_A) of 300 and 375°C. The resulting phase distributions of treated specimens were characterised using X-Ray Diffraction (XRD) method. The patterns of XRD were found to consist of ferrite (α) and austenite (γ) phases. The percentage volume of carbon-enriched stabilised austenite in the ADI decreased as section thickness increased. It was concluded that the carbon-enriched stabilised austenite in ADI depends on the casting section thickness and austempering temperature.

Keywords: Ductile iron; Aaustempered ductile iron; Carbon stabilised austenite; Acicular ferrite; Casting thickness

1. INTRODUCTION

Austempered ductile iron has an optimum combination of high strength and ductility, resistance to wear, toughness and fatigue strength (Yang and Putatunda, 2004; Harding, 2005; Keough and Hayrynen, 2006; Artola *et al*., 2017; Zanardi *et al*., 2017). As a result of the combination of these favourable properties, it is used for structural applications in machine building, automobile assembly, war implements and construction machineries (Yang and Putatunda, 2004; Keough and Hayrynen, 2006; Zimba, 2003; Tun and Lwin, 2008; Bixler *et al*., 2010; Justin and Keough, 2010). These pleasant mechanical properties are possible because ADI structure is a mixture of carbon-enriched stabilised austenite which imparts ductility, and acicular ferrite which imparts strength (Ronus, 1984; Kovacs and Keough, 1993; Kovacs, 1994; Erić *et al*., 2004; Basso and Sikora, 2012). Thus, the structural form of acicular ferrite, percentage volume fraction of carbon-enriched stabilised austenite, and quantity of carbon in the carbon-enriched stabilised austenite are important microstructural features of ADI. These distinguish microstructures determine the ADI mechanical properties, while the austempering variables (austempering temperature and time) determine the structural form (Erić *et al*., 2006). The matrix mixture of carbon-enriched stabilised austenite and acicular ferrite gives ADI superior mechanical properties (Erić *et al*., 2004; Basso and Sikora, 2012; Olawale *et al*., 2017) when compared it with ductile iron that has pearlite or ferrite matrix (Samuel and Viswanathan, 2008). However, the austempering variables determine the proportion of these two phases in the ADI matrix.

Austempered ductile iron undergo two-stage reaction during austempering transformation. During the first stage, austenite breaks down into acicular ferrite (α) and carbon-enriched stabilised austenite (γHC). Ferrite nucleates and grow into austenite during the transformation process. The nucleation of ferrite leads to rejection of carbon into the surrounding austenite and as a result austenite becomes enriched with carbon (Yang and Putatunda, 2004; Swain *et al*., 2012; Górny *et al*., 2014). The enrichment of austenite with carbon becomes increases as more and more ferrite nucleates. At this stage the austenite contains carbon content exceeding 1.0% which is thermally stable at room temperature. Hence, the final microstructure consists of a matrix mixture of ferrite and carbon-enriched stabilised austenite, and dispersed graphite nodules (Putatunda, 2001; Konečná *et al*., 2011; Yusuf and Yılmaz, 2011; Méndez *et al*., 2017). Austempered ductile iron has remarkable properties because of this structure.

If the casting is austempered longer than required, then second stage transformation will commence, where the carbon-enriched stabilised austenite will breaks down into ferrite and ε-carbide. The presence of -carbide after second reaction makes the materials to becomes brittles and affects the mechanical properties of ADI, hence, it must be avoided (Amar, 2012; Costaa *et al*., 2010). The time between the end of the first reaction and the beginning of the second reaction is referred to as the 'process window' (Bahmani and Elliot, 1994; Yescas *et al*., 2001).

Copyright Reserved © NJMSE, 2017.

The microstructural feature of ADI can be optimised between this window. A short austempering time will lead to formation of martensite because austenite will be inadequately enriched and subsequently lower the carbon content in stabilised austenite. If the austempering time is beyond the time for commencement of second stage there will be formation carbide precipitate and again, a reduction in the carbon content of carbon-enriched stabilised austenite. The austempering period between process window will lead to the formation of ausferrite matrix. This structure is the mixture of carbon-enriched austenite (γHC) and acicular ferrite (α). The excellent mechanical properties attributed to ADI is as a results this unique matrix (Bahmani and Elliot, 1994; Yescas *et al*., 2001).

Several investigations have reported the effects of austempering temperature and time on the carbon-enriched stabilised austenite (Grny *et al*., 2014; Bayati and Elliot, 1997; Rao and Putatunda, 2003; Vikas *et al*., 2008; Vaško, 2009; Amran *et al*., 2010; Vaško, *2011;* Erfanian-Naziftoosi, 2012; Atanda *et al*., 2014). However, the focus of this study is the effect of casting section thickness on the quantity of carbon-enriched stabilised austenite which to the best of our knowledge has not been investigated.

2. MATERIALS AND METHOD

The ASTM A536 65-45-12 (1998) grade of ductile iron used in this work was cast using facilities available in Nigerian Foundries Limited, Sango-Ota, Ogun State, Nigeria. The charge makes up consisting of steel scrap (65%), recycle ductile iron (20%) and pig iron (15%) were melted inside 500 kg medium frequency (3000 Hz) induction furnace. Deficiencies in the chemical composition was adjusted by adding petroleum coke and 75 wt.% ferrosilicon. To ensure homogenisation the melt was superheated to 1550°C and thereafter spheroidised at 1450°C. Tundish ladle process was used to perform spheroidisation treatment using a Fe-Si-5.5%Mg alloy. This was followed by post inoculation with 0.6 percent weight granule of 75 wt.% ferrosilicon, after which the melt was poured at 1440°C into green sand molds with a Y-block shape in accordance with ASTM A897/897M-16 standard (2016). The chemical composition of the casting was analysed by photospectrometry. The final chemistry was presented in Table 1.

From the leg part of the Y-blocks, flat specimens of 25 by 80 mm of 5, 10, 15, 20 and 25 mm thickness were machined and from which ADI were produced by an isothermal heat treatment. The heat treatment involved two steps that consisted of austenitising and austempering. The specimens were austeinitised at a temperature of 820°C and were held at the temperature for a period of 1 h for complete austenitisation of the structure. They were then rapidly quenched into a salt bath maintained at temperatures of 300 and 375°C and were held isothermally at these temperatures for 2 hrs. The specimens were finally air cooled to room temperature.

X-ray diffraction (XRD) method was used to characterised the morphology of the microstructure and phase distribution of as cast and heat treated specimens. A monochromatic Kα radiation of cobalt at 100 mA and 40 kV was used for the X-ray diffraction analysis. The angular 2θ was scanned at a speed of 0.25 and 1° per minute in the range of 30 - 110° and 45 - 120° respectively using Rigaku rotating head anode diffractometer. The profiles were thereafter analysed using a PANalytical X'Pert Pro powder diffractometer in θ-θ configuration with an X'Celerator detector and variable divergence and fixed receiving slits with Fe filtered Co-Kα radiation (λ=1.789Å). Thereafter X'Pert Highscore Plus Software was used for the identification of phases present in the specimens. The integrated intensities and peak positions of (311), (220) and (111) planes of austenite and (211) and (110) planes of BCC ferrite were also obtained from the profile.

The fraction of the carbon-enriched stabilised austenite (X_γ) was evaluated using X-ray diffraction technique (Miller, 1978) according to Equations (1) - (3).

$$X_\gamma = 1.4I_\gamma/(I_\alpha + 1.4I_\gamma) \quad \text{.....(1)}$$

where

$$I_\gamma = (I_\gamma^{220} + I_\gamma^{211})/2 \quad \text{.....(2)}$$

and

$$I_\alpha = I_\alpha^{211} \quad \text{.....(3)}$$

where $I_{\gamma,\alpha}^{hkl}$ is the reflected intensity of the *hkl* of the respective phase.

Also, lattice parameters of the austenite (a_γ) were determined by X-ray measurements. The position of the diffraction peaks was determined and converted to diffracted angles using standard techniques (Cullity, 1978). From the values of lattice parameters, the carbon-enriched stabilised austenite (C_γ) was computed according to Equation (4) (Ronus and Rundman, 1987).

$$C_\gamma = (a_\gamma - 0.3548)/0.00441 \quad \text{.....(4)}$$

At the austenitising temperature the carbon content in the parent austenite (C_o) is fixed and was obtained by Equation (5) (Voigt and Loper, 1984):

$$C_o = T_\gamma/420 - 0.17(\%Si) - 0.95 \quad \text{.....(5)}$$

where T_γ is the austenitising temperature in °C. This carbon (C_o) was distributed between the ferrite and austenite. Therefore,

$$C_o = X_\alpha C_\alpha. + X_\gamma C_\gamma \quad \text{.....(6)}$$

where X_α is the fraction of acicular ferrite in volume, C_α is the carbon content of acicular ferrite, X_γ is the

Copyright Reserved © NJMSE, 2017.

Table 1: The results of chemical composition of ductile iron produced compared with standard ASTM A536 65-45-12 grade

Elements	%C	%Si	%Mn	%P	%S	%Mg
Standard Value	3.5 – 4.0	2.2 – 2.9	0.3 – 0.6	0.05 max	0.25 max	0.02 – 0.06
Measured Value	3.61	2.54	0.40	0.017	0.023	0.05

fraction of carbon-enriched stabilised austenite in volume, and C_γ is the carbon content of carbon-enriched stabilised austenite. Since carbon dissolved by ferrite is very little ($C_\alpha \approx 0.002$), the carbon content of parent austenite was estimated according to Equation (7).

$$C_o = X_\gamma C_\gamma \quad \text{.....(7)}$$

The beginning of martensite transformation, M_s, was estimated using chemical composition of the material, empirical equations from literature, and isopleths through Fe-C-2.5 wt.%Si phase diagram (Ronus and Rundman, 1987). The Ms temperature in °C was estimated as a function of weight percent of the carbon content (C_0) present in parent austenite according to Equation (8).

$$Ms = 400 - 260C_0 \quad \text{.....(8)}$$

Due to the presence of manganese, nickel, chromium, molybdenum and silicon in the chemical composition, the M_s value is somewhat lower. Hence, different expressions based on the alloying element, were used to estimate the Ms temperature. The expression due to Lui *et al.* (2001) and Silva *et al.* (2014) was considered. In this expression the coefficient due to manganese, nickel, chromium, molybdenum and silicon contents are 30.4, 17.7, 12.1, 7.5 and 7.5 respectively. Hence, the estimate of Ms was made according to Equation (9):

$$Ms = 400 - 260C_0 - 30.4Mn - 17.7Ni - 12.1Cr - 7.5Mo - 7.5Si \quad \text{.....(9)}$$

3. RESULTS AND DISCUSSION

The X-ray diffraction patterns of the specimens for different section thickness are as presented in Figures 1 and 2. The peaks of diffraction existed in 2 ranges from 50.2 - 109.5° which were identified as γ(111), α(110), γ(002), α(200), γ(220), α(211) and γ(311). These peaks correspond to Bragg angles of 50.2°, 52.3°, 58.4°, 77.1°, 88.5°, 99.7° and 109.5° respectively.

The patterns predominantly consisted of peak values of austenite (γ) and ferrite (α) phases which are located near to each other. This suggests the formation of a matrix comprised of a mixture of carbon-enriched stabilised austenite and acicular ferrite often referred to as ausferrite.

The volume fraction of carbon-enriched stabilised austenite (X_γ) and acicular ferrite (X_α) were determined using Equations (1) to (3) and the results obtained are shown in Table 2. The carbon content of the stabilised austenite (C_γ) was estimated according to Equation (4) and the result obtained is shown in Table 3. The content of carbon present in the parent austenite (C_o) at the austenitising temperature was estimated to be 0.571 wt.% (Equation 5). The corresponding temperature of the beginning of martensite transformation, Ms, was estimated to be 219°C using Equation (9). The total carbon in the carbon-enriched stabilised austenite ($X\gamma C_\gamma$) was estimated according to Equation (7) and result is shown in Table 4. The summary of the X-ray diffraction analysis for all the investigated ADI specimens are shown in Table 5.

The volume fraction variation of carbon-enriched stabilised austenite and acicular ferrite with austempering temperatures and casting section thicknesses are shown in Figure 3(a) and (b). From the results the volume fraction of carbon-enriched stabilised austenite decreases steadily with increasing section thickness while acicular ferrite increase with increasing section thickness. Figure 4 shows the effects of austempering temperature on the carbon content of austenite while a change in total carbon in carbon-enriched stabilised austenite is presented in Figure 5.

From Figure 3(a), the austenite content was observed to be higher at high austempering temperature. The trends of volume fraction variation of carbon-enriched stabilised austenite with section thickness were similar in the two investigated austempering temperatures (300 and 375°C). However, at T_A of 375°C the volume fraction of carbon-enriched stabilised austenite was relatively higher by 18% when compared with T_A of 300°C. Ferrite nucleates out of austenite during the austenitising process, dissolves very little carbon (0.002%), and the dissolves carbon diffuse out into the surrounding austenite in order for the ferrite to grow (Tanmoy and Goutam, 2018). Since nucleation depends on the degree of supercooling, the lower the austempering temperature the higher the degree of supercooling and the more theferrite that will be nucleated (Putatunda, 2001; Yang and Putantuda, 2004). However, at the high degree of supercooling diffusion rate of carbon becomes lower and the rate of growth of ferrite slowed down. This is the reasonwhile the quantity of ferrite is more at of 300°C (Figure 3b). At T_A of 375°C the nucleation of ferrite was less because of the lower degree of supercooling, diffusion rate of carbon becomes higher, and the rate of grow of ferrite becomes faster. This is the reason the quantity of ferrite is less at T_A of 375°C (Figure 3b). Thus, at T_A of 300°C the volume fraction of ferrite (X_α) was more than volume fraction of carbon-enriched stabilised austenite (X_γ) while at T_A of 375°C X_γ was greater than X_α.

Copyright Reserved © NJMSE, 2017.

Table 2: Percentage volume fraction of carbon-enriched stabilised austenite

Section Thickness (mm)	Austempering Temperature (°C)	I_γ^{220}	I_γ^{311}	$I_\alpha = I_\alpha^{211}$	$X_\gamma = \frac{I_\gamma^{220} + I_\gamma^{311}}{2}$	% X_γ
5	300	15.55	2.99	9.270	0.3241	32.41
	375	2.73	3.47	3.100	0.4003	40.03
10	300	4.10	0.84	2.470	0.2842	28.42
	375	3.24	6.03	4.635	0.3347	33.47
15	300	1.91	2.76	2.335	0.2532	25.32
	375	10.56	2.29	6.425	0.2860	28.60
20	300	3.58	3.91	3.745	0.2061	20.61
	375	4.57	3.91	4.240	0.2521	25.21
25	300	3.92	2.13	3.025	0.1537	15.37
	375	0.60	4.50	2.550	0.1744	17.44

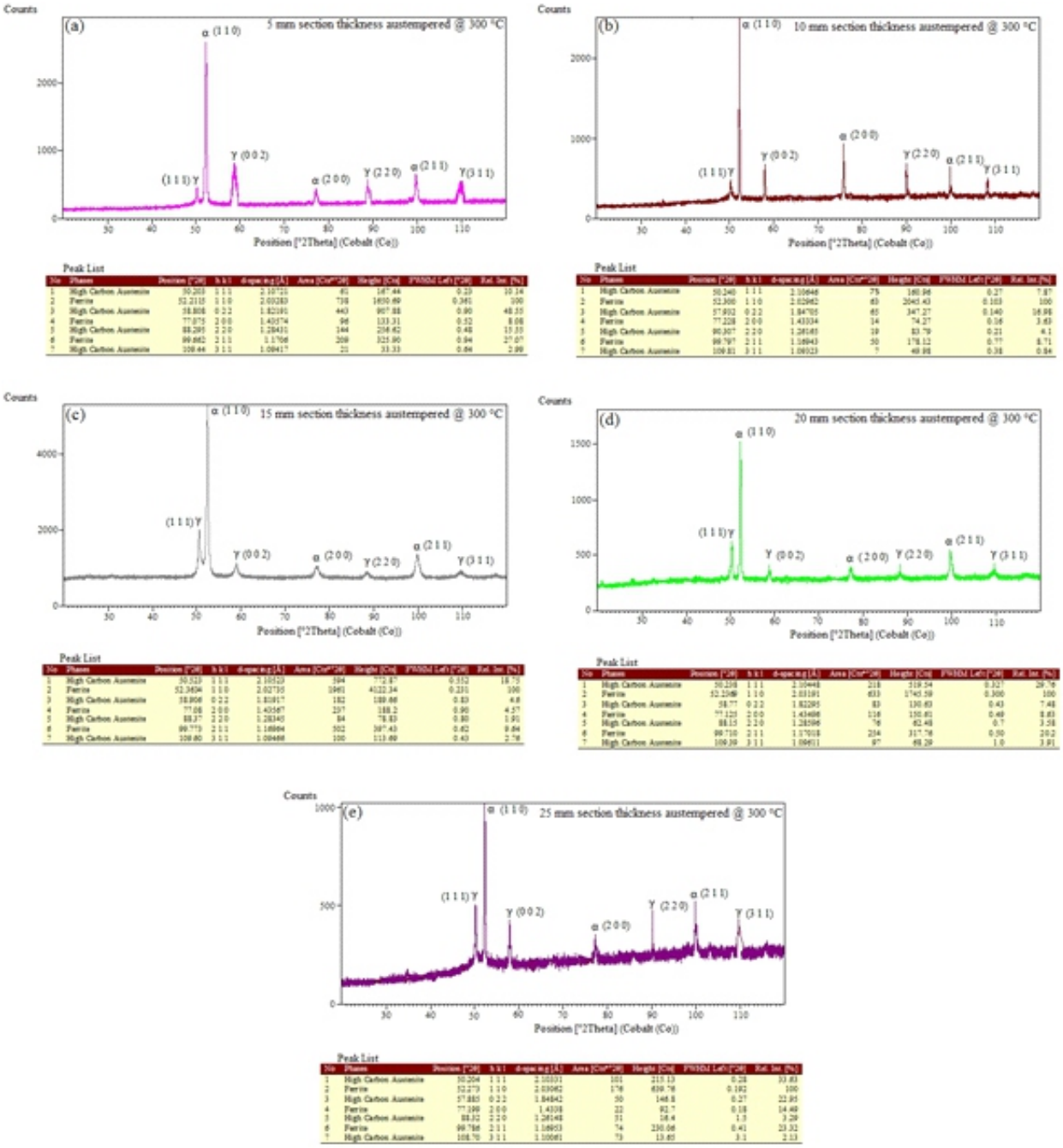

Figure 1: X-ray diffraction pattern of (a) 5, (b) 10, (c) 15, (d) 20 and (e) 25 mm section thickness austempered at 300°C

Copyright Reserved © NJMSE, 2017.

Table 3: Carbon content of carbon-enriched stabilised austenite

Section Thickness (mm)	Austempering Temperature (°C)	d-spacing of (111) peak of Austenite (nm)	$h\ k\ l$	Lattice Parameter $a_\gamma = d\sqrt{h^2+k^2+l^2}$	Carbon Content of Carbon-Enriched Stabilised Austenite $c_\gamma = \frac{a_\gamma - 0.3548}{0.00441}$
5	300	0.210721	1 1 1	0.3650	2.31
	375	0.210992	1 1 1	0.3654	2.40
10	300	0.210646	1 1 1	0.3648	2.27
	375	0.210961	1 1 1	0.3653	2.38
15	300	0.210523	1 1 1	0.3646	2.22
	375	0.210857	1 1 1	0.3652	2.36
20	300	0.210448	1 1 1	0.3645	2.20
	375	0.210793	1 1 1	0.3651	2.34
25	300	0.210331	1 1 1	0.3643	2.15
	375	0.210731	1 1 1	0.3650	2.31

Table 4: Total carbon of carbon-enriched stabilised austenite

Section Thickness (mm)	Austempering Temperature (°C)	Volume Fraction of Carbon-Enriched Stabilised Austenite (X_γ)	Carbon Content of Carbon-Enriched Stabilised Austenite (C_γ)	Total Carbon of Carbon-Enriched Stabilised Austenite ($X_\gamma C_\gamma$)
5	300	0.3241	2.31	0.7486
	375	0.4003	2.40	0.9607
10	300	0.2842	2.27	0.6451
	375	0.3347	2.38	0.7966
15	300	0.2532	2.22	0.5621
	375	0.2860	2.36	0.6750
20	300	0.2061	2.20	0.4534
	375	0.2521	2.34	0.5899
25	300	0.1537	2.15	0.3305
	375	0.1744	2.31	0.4029

Table 5: Results of x-ray diffraction analysis of investigated ADI

Section Thickness (mm)	Austempering Temperature (°C)	Volume Fraction of Acicular Ferrite (X_α)	Volume Fraction of Carbon-Enriched Stabilised Austenite (X_γ)	Carbon Content of Carbon-Enriched Stabilised Austenite (C_γ)	Total Carbon of Carbon-Enriched Stabilised Austenite ($X_\gamma C_\gamma$)
5	300	0.6759	0.3241	2.31	0.7486
	375	0.5997	0.4003	2.40	0.9607
10	300	0.7158	0.2842	2.27	0.6451
	375	0.6653	0.3347	2.38	0.7966
15	300	0.7468	0.2532	2.22	0.5621
	375	0.7140	0.2860	2.36	0.6750
20	300	0.7939	0.2061	2.20	0.4534
	375	0.7479	0.2521	2.34	0.5899
25	300	0.8463	0.1537	2.15	0.3305
	375	0.8256	0.1744	2.31	0.4029

Copyright Reserved © NJMSE, 2017.

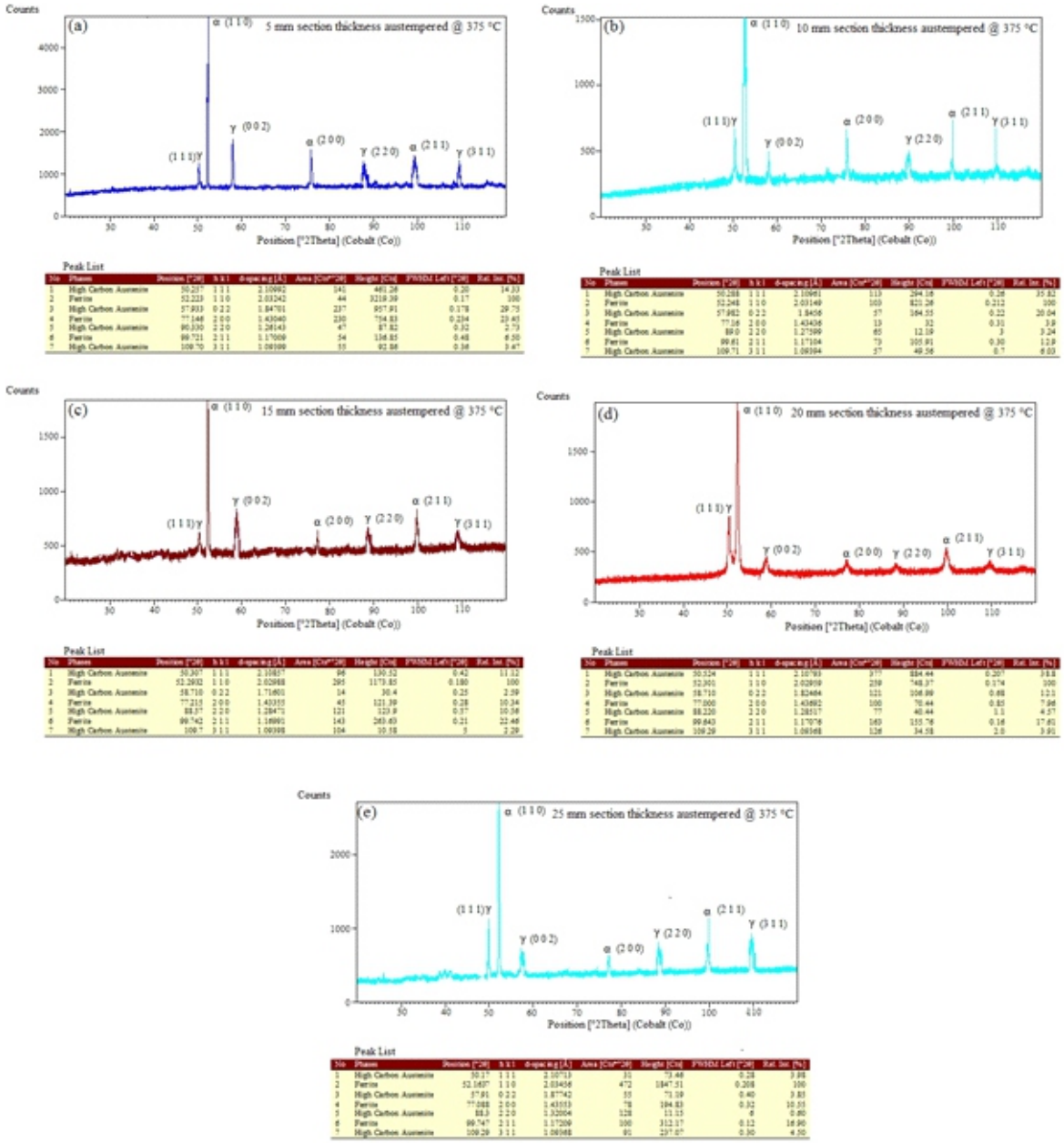

Figure 2: X-ray diffraction pattern of (a) 5, (b) 10, (c) 15, (d) 20 and (e) 25 mm section thickness austempered at 375°C

At austenitising temperature of 820°C the M_s temperature as estimated by Equation (9) was 219°C. This temperature was lower than the austempering temperatures considered in this study and hence there was no room for austenite to transform to martensite. Due to the high temperature difference between T_A of 375°C and M_s, large amount of austenite was enriched with carbon while cooling to room temperature. This explained the reason why the volume fraction of X_γ was relatively higher by about 18% at T_A of 375°C than T_A of 300°C.

As evident from Figure 4 the carbon content of the stabilised austenite (C_γ) at T_A of 375°C was more than that at T_A of 300°C. The austempering carried out at T_A of 375°C produced higher austenitic carbon content ($X_\gamma C_\gamma$) than the one at 300°C. At a high T_A, the carbon content of the austenite increases because diffusion rate of carbon is high at this temperature (Putantuda, 2001). Since diffusion depend on temperature, diffusion rate of carbon was high at T_A of 375°C which resulted in carbon partitioning, and consequently higher $X_\gamma C_\gamma$. The value of $X_\gamma C_\gamma$ is important because it can be taken as the total carbon in the carbon-enriched stabilised austenite. From Figure 5, the value of austenitic carbon content ($X_\gamma C_\gamma$) decreased as the section thickness increased for each of the investigated austempering temperature, however, at T_A of 375°C

Copyright Reserved © NJMSE, 2017.

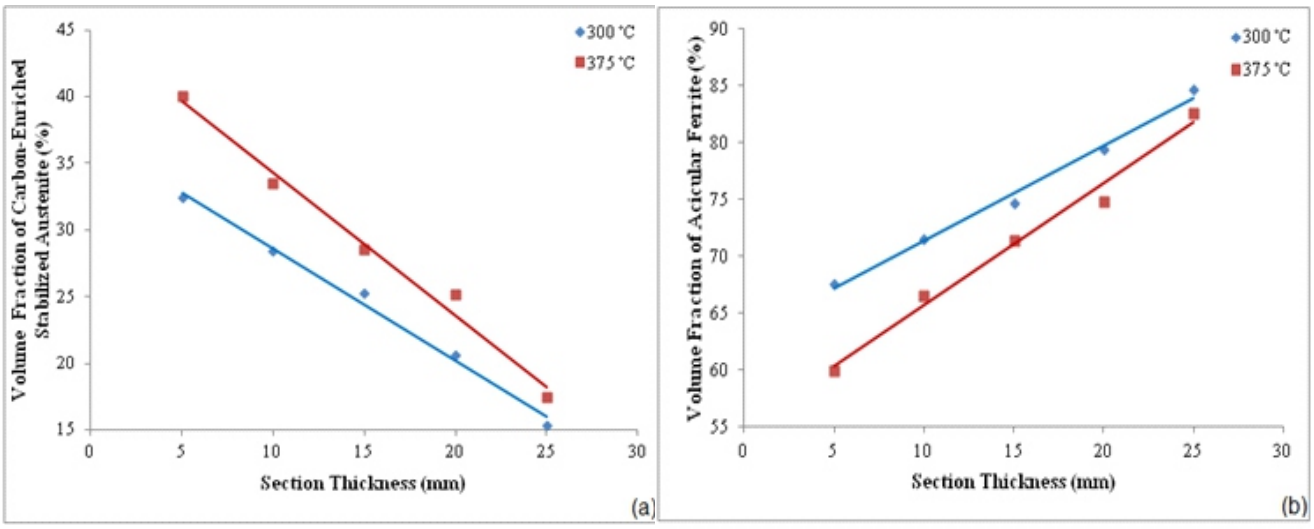

Figure 3: Influence of section thickness on volume fraction of (a) carbon-enriched stabilised austenite and (b) acicular ferrite at different austempering temperature

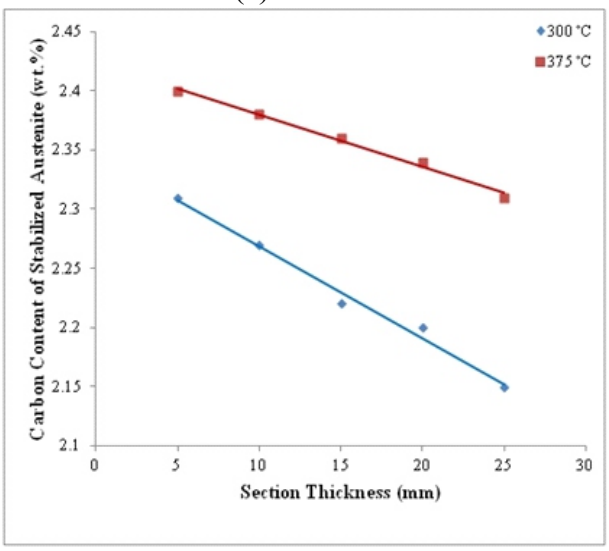

Figure 4: Influence of section thickness on the carbon content of carbon-enriched stabilised austenite (C_γ) at different austempering temperature

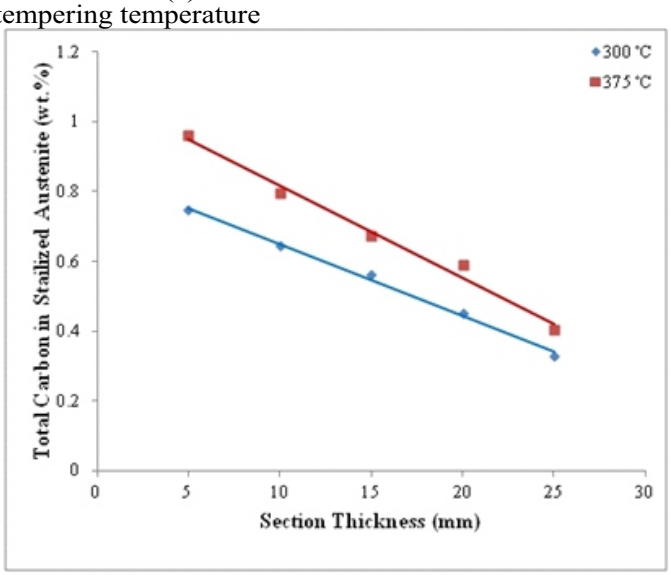

Figure 5: Influence of section thickness on the total carbon in the carbon-enriched austenite ($X_\gamma C_\gamma$) at different austempering temperature

this value was more compared to that of T_A of 300°C for all the section thickness investigated. Since both carbon-enriched stabilised austenite content and its carbon content were higher at T_A of 375°C for all the section thickness, $X_\gamma C_\gamma$ was accordingly higher. However, $X_\gamma C_\gamma$ decreased as the section thickness increased. At T_A of 375°C, C_γ and $X_\gamma C_\gamma$ were higher than that of 300°C by about 6% and 25% respectively.

It was observed in this study that T_A of 375°C resulted in higher percentage volume of carbon-enriched stabilised austenite (X_γ), carbon content in austenite (C_γ) and total carbon content ($X_\gamma C_\gamma$) for all ranges of section thickness than those obtained at T_A of 300°C. On the other hand, percentage volume of acicular ferrite (X_α) is higher at T_A of 300°C than those obtained at T_A of 375°C. However, the amount of carbon-enriched stabilised austenite decreased with increase in section thickness while the amount of acicular ferrite increased.

4. CONCLUSION

It can be concluded from this study that the fraction of volume of carbon-enriched stabilised austenite and acicular ferrite in ADI depends on the section thickness of casting and austempering temperature. Volume fraction of stabilised austenite decreases with increase in section thickness but increases with austempering temperature. Also, total carbon content and carbon of carbon-enriched stabilised austenite decreases with increase in section thickness but increases with austempering temperature. However, the volume

Copyright Reserved © NJMSE, 2017.

fraction of acicular ferrite in austempered ductile iron increases with the section thickness while it decreases with austempering temperature.

ACKNOWLEDGEMENTS

This work was technically supported by Nigerian Foundries Limited, Sango-Ota, Ogun State, Nigeria. The authors are sincerely grateful for their contribution.

REFERENCES

Amar, K.D. (2012), "Variation of mechanical properties of austempering ductile iron with processing parameters", International Journal of Current Research, 4(8): 012 016.

Amran, Y., Katsman, A., Schaaf, P. and Bamberger M. (2010), "Influence of copper addition and temperature on the kinetics of austempering in ductile iron", Metallurgical and Materials Transactions B, 41B: 1052-1058.

Artola, G. Gallastegi, I. Izaga, J. Barrea M. and Rimmer, A. (2017), "Austempered ductile iron (ADI) alternative material for high-performance applications", International Journal of Metalcasting, 11(1): 131135.

ASTM A 536 (1998), "Ductile iron casting specific: TensileYieldElongation", American Society for Testing and Materials International, West Conshohocken, PA., 1(2): 321 325.

ASTM A897/897M-16 (2016), "Standard specification for austempered ductile iron castings", American Society for Testing and Materials International, West Conshohocken, PA. www.astm.org.

Atanda, P.O., Olorunniwo, O.E. and Imasogie, B.I. (2013), "Effect of process parameters on the mechanical properties of iso-thermal treated ductile iron", Materials Performance and Characterization, 3(1): 255-264.

Basso, A. and Sikora, J. (2012), "Review on production processes and mechanical properties of dual phase austempered ductile iron", International Journal of Metalcasting, 6(1):714.

Bahmani, M. and Elliot, R. (1994), "Isothermal transformation diagrams for alloyed ductile iron cast iron", Materials Science and Technology, 10:1068-1072.

Bayati, H. and Elliot R. (1997), "Role of austenite in promoting ductility in an austempetred ductile iron", Materials Science and Technology, 13:319-325.

Bixler, C., Hayrynen, K., Keough, J., Pfaffmann, G. and Gledhill, S. (2010), "Locally austempered ductile iron (LADI)", Society of Automotive Engineers International, 2010-01-0652.

Costaa, N., Machadob and Silvaa, F.S. (2010), "A new method for prediction of nodular cast iron fatigue limit", International Journal of Fatigue, 32(7):988995.

Cullity, B.D. (1978). Elements of x-ray diffraction, 2nd ed., Massachusetts: Addison-Wesley Company Incorporated.

Erfanian-Naziftoosi, H.R., Haghdadi, N. and Kiani-Rashid, A.R. (2012), "The effect of isothermal heat treatment time on the microstructure and properties of 2.11% Al austempered ductile iron", Journal of Materials Engineering and Performance, 21(8):1785-1792.

Erić, O., Jovanovic, M., Šidjanin, L. and Rajnovic, D. (2004), "Mechanical properties of CuNiMo austempered ductile iron", Journal of Mining and Metallurgy, 40B(1):11-19.

Erić, O., Rajnovic, D., Zec, S., Sidjanin, L. and Jovanovic, M.T. (2006), "Microstructure and fracture of alloyed austempered ductile iron", Materials Characteristic, 57:211 217.

Grny, M, Tyrała, E. and Lopez, H. (2014), "Effect of copper and nickel on the transformation kinetics of austempered ductile iron", Journal of Materials Engineering and Performance, 23(10):3505-3510.

Harding, R.A. (2005), "The production, properties and automotive for austempered ductile iron", Asia-Europe Environment Forum Conference, Jakarta, Indonesia, November 23-25, 2005.

Justin, L. and Keough, J.R. (2010), "Austempering materials for powertrain application", Applied Process Inc. Technologies Div. - Livonia, Michigan, USA.

Keough, J.R. and Hayrynen, K.L. (2006), "Developments in the technology and engineering application of austempered ductile iron (ADI)", Proceedings of the 8th International Symposium on Science and Processing of Cast Iron, Beijing, China, October 16 19, 2006:474-479.

Konečná, R., Kokavec, M. and Nicoletto, G. (2011), "Influence of surface quality on fatigue behavior of nodular cast iron", Procedia Engineering, 10: 25382543.

Kovacs, B. (1994), On the terminology and structure of ADI", America Foundry Society Transactions, 56:417-420.

Kovacs, B. and Keough, J. (1993), "Physical properties and application of austempered gray iron", America Foundry Society Transactions AFS, 93-141:283-291.

Lui, C., Zhao, Z., Northwood D.O. and Lui, Y. (2001), "A new empirical formula for calculation of temperatures in pure iron and super-low carbon alloy steels", Journal of Materials Processing Technology, 113(1-3): 556-562.

Méndez, S., de la Torre, U., González-Martínez, R. and Sarez, R. (2017), "Advanced properties of ausferritic ductile iron obtained in as-cast conditions", International Journal of Metalcasting, 11(1):116122.

Moore, D.J., Ronus, T.N. and Rundman, K.B. (1987), "The relationship between microstructure and tensile properties in ADI", American Foundry Society Transactions, 95:765-774.

Miller, R.L. (1964). Transaction of ASM, 57:892-899.

Olawale, J.O., Ibitoye, S.A., Oluwasegun, K.M., Shittu, M.D. and Popoola, A.P.I. (2017), "A novel technique for austempered ductile iron production", International Journal of Metalcasting, 11(3):568580.

Putatunda, S.K. (2001), "Development of austempered ductile cast iron (ADI) with simultaneous high yield strength and fracture toughness by a novel two-step austemperingprocess", Materials Science and Engineering, A315:70-80.

Rao, P.P. and Putatunda, S.K. (2003), "Investigations on the fracture toughness of austempered ductile irons austenitised at different temperatures", Materials Science and Engineering, A349:136 -149.

Ronus, T.N. and Rundman, K.B. (1987), "Constitution of austempered ductile iron and kinetics of austempering", American Foundry Society Transactions, 95:851-874.

Copyright Reserved © NJMSE, 2017.

Ronus, T.N., Rundman, K.B. and Moore, D.J. (1984), On the structure and properties of austempered ductile cast iron", American Foundry Society Transactions, 121:815-840.

Samuel, C. and Viswanathan, S. (2008), "Transformation kinetics and ferrite-pearlite ratios in a 65-45-12 ductile iron", International Journal of Metalcasting, 2(4):5565.

Silva, A.J.S.T., Goldenstein, H., Guesser, W.L. and Campos, M.F. (2014), "Quenching and partitioning heat treatment in ductile cast irons", Materials Research, 17(5):1115-1123.

Swain, S.K., Panda, R.K., Dhal, J.P., Mishra, S.C. and Sen, S. (2012), "Phase investigation of austempered ductile iron", Orissa Journal of Physics, 19(1):173-180.

Tanmoy S., Goutam S. (2018):"Relationship between matrix-microstructure and mechanical properties of copper alloyed thin wall austempered gray cast iron (TWAGI)", International Journal of Cast Metals Research, 31(1):20 28.

Tun, T. and Lwin, K.T. (2008), "Optimizing the micro-structure and mechanical properties of austempered ductile iron for automobile differential gear", Journal of Metals, Materials and Minerals, 18(2):199-205.

Vaško, A. (2009), "Chosen factors influencing micro-structure and mechanical properties of austempered ductile iron", Materials Engineering, 16(4):11-15.

Vaško, A. (2011), "Influence of transformation temperature on structure and mechanical properties of austempered ductile iron", Acta Metallurgica Slovaca, 17(1):45-50.

Vikas, C., Uma, B., Puri, D. and Amita, C. (2008), "To Study the effect of austempering temperature on fracture behaviour of Ni-Mo austempered ductile iron (ADI)", Journal of Minerals and Materials Characterization and Engineering, 7(4):307-316.

Voigt, R.C. and Loper, C.R. (1984), "Austempered ductile iron process control and quality assurance", Journal of Heat Treament, 3: 291-309.

Yang, J. and Putatunda, S.K. (2004), "Influence of a novel two-step austempering process on the strain-hardening behavior of austempered ductile cast iron (ADI)", Materials Science and Engineering A, 382(1-2): 265 279.

Yang J., Putatunda S.K. (2004), "Improvement in strength and toughness of austempered ductile cast iron by a novel two step austempering process", Materials and Design, 25(3):219-230.

Yescas, M.A., Bhadeshia, H.K.D.H. and MacKay, D.J. (2001), "Estimation of the amount of retained austenite in austempered ductile irons using neural networks", Materials Science and Engineering, A311:162 -173.

Yusuf, K. and Yılmaz, Y. (2011), "The effects of boro-tempering heat treatment on microstructural properties of ductile iron", Materials and Design, 32:14141419.

Zanardi, F., Bonollo, F., Angella, G., Bonora, N., Iannitti, G. and Ruggiero, A. (2017), "A contribution to new material standards for ductile irons and austempered ductile irons", International Journal of Metalcasting, 11(1):136147.

Zimba, J. Simbi, D.J. and Navara, E. (2003), "Austempered ductile iron: an alternative material for earth moving components", Cement and Concrete Composites, 25:643-649.

Copyright Reserved © NJMSE, 2017.